OPEN ACCESS Freely available online

PLOS ONE

Muscular Weakness in Individuals with HIV Associated with a Disorganization of the Cortico-Spinal Tract: A Multi-Modal MRI Investigation

Charlotte Bernard[1,2,3], Bixente Dilharreguy[1,2], Michèle Allard[1,2,3,5], Hélène Amieva[4], Fabrice Bonnet[4,5], Frédéric Dauchy[5], Carinne Greib[5], Patrick Dehail[5,6], Gwénaëlle Catheline[1,2,3]* for the ANRS CO3 Aquitaine cohort study group[¶]

1 Université de Bordeaux, INCIA, UMR 5287, Talence, France, **2** CNRS, INCIA, UMR 5287, Talence, France, **3** EPHE, Bordeaux, France, **4** Université Bordeaux Segalen, INSERM U 897, ISPED, Bordeaux, France, **5** Centre Hospitalier Universitaire (CHU), Bordeaux, France, **6** Université de Bordeaux, EA 4136, Bordeaux, France

Abstract

Motor impairment is highly prevalent in HIV-infected patients. Here, we assess associations between peripheral muscular deficits as evaluated by the 5 sit-to-stand test (5STS) and structural integrity of the motor system at a central level. Eighty-six HIV-infected patients receiving combination antiretroviral therapy and with no major cerebral events, underwent an MRI scan and the 5STS. Out of 86 participants, forty presented a score greater than two standard deviations above mean normative scores calculated for the 5STS and were therefore considered as motor-impaired. MRI-structural cerebral parameters were compared to the unimpaired participants. Fractional Anisotropy (FA), Axial Diffusivity (AD) and Radial Diffusivity (RD), reflecting microstructural integrity, were extracted from Diffusion-Tensor MRI. Global and regional cerebral volumes or thicknesses were extracted from 3D-T1 morphological MRI. Whereas the two groups did not differ for any HIV variables, voxel-wise analysis revealed that motor-impaired participants present low FA values in various cortico-motor tracts and low AD in left cortico-spinal tract. However, they did not present reduced volumes or thicknesses of the precentral cortices compared to unimpaired participants. The absence of alterations in cortical regions holding motor-neurons might argue against neurodegenerative process as an explanation of White Matter (WM) disorganization.

Citation: Bernard C, Dilharreguy B, Allard M, Amieva H, Bonnet F, et al. (2013) Muscular Weakness in Individuals with HIV Associated with a Disorganization of the Cortico-Spinal Tract: A Multi-Modal MRI Investigation. PLoS ONE 8(7): e66810. doi:10.1371/journal.pone.0066810

Editor: Alejandro Lucia, Universidad Europea de Madrid, Spain

Received January 24, 2013; **Accepted** May 12, 2013; **Published** July 11, 2013

Funding: This study was supported by grants from the French Agency for AIDS and hepatitis research (ANRS). The funders had no role in study design, data collection and analysis, decision to publish, or preparation of the manuscript.

Competing Interests: The authors have declared that no competing interests exist.

* E-mail: gwenaelle.catheline@u-bordeaux2.fr

¶ Membership of the ANRS CO3 Aquitaine cohort study group is provided in the Acknowledgments.

Introduction

The use of combination antiretroviral therapy (cART) has drastically improved the prognosis and the quality of life of patients infected with human immunodeficiency virus (HIV). However, neurological impairments and specifically neuromuscular problems remain highly prevalent in this population despite better control of HIV replication. These muscular impairments are also associated with daily activity limitations and participation restrictions [1,2]. The most common motor impairments in AIDS patients are slowed movements, gait abnormality, limb incoordination, hyperreflexia, hypertonia, and muscular weakness [3,4]. Consistent with these observation, we have shown [5] that half of adults with controlled HIV-infection had poor lower limb muscle performance as assessed through 5-Sit-To-Stand test (5STS) [6]. Given that performance on the 5STS test has been related to falls in older adults [7–9], HIV-1 participants infected individuals presenting poor 5STS performance should be considered as being at risk for falls.

Using MRI, several studies have demonstrated that HIV patients present White Matter (WM) alterations [10,11]and psychomotor slowing and postural instability in HIV patients are related to these modifications [12–14]. In addition, finger tapping performance in this population were associated to the microstructural integrity of whole cerebrum white matter [13] as well as to the splenium of the corpus callosum [12], whereas balance scores were related to pontocerebellar tract integrity [14]. Moreover, chronic infection with HIV has been associated with skeletal muscle impairment [15–18], which is related to deterioration of functional ability in activities of daily living [19]. Whereas muscle weakness is well-known in the disease process, its relationship to central motor command integrity has not been investigated to date.

Taking into account these observations, we hypothesize that muscular deficits are selectively associated with central motor bundle integrity in HIV patients. In this investigation, we used Diffusion Tensor Imaging (DTI) to analyze white matter bundle microstructural organization in HIV patients presenting muscular deficits on the 5STS and compared them to unimpaired patients. These measures were evaluated through Fractional Anisotropy (FA), extracted from DTI [20,21]. DTI is based on water motions which are differently constrained according to tissue architecture; in WM water diffusion was preferentially constrained in the

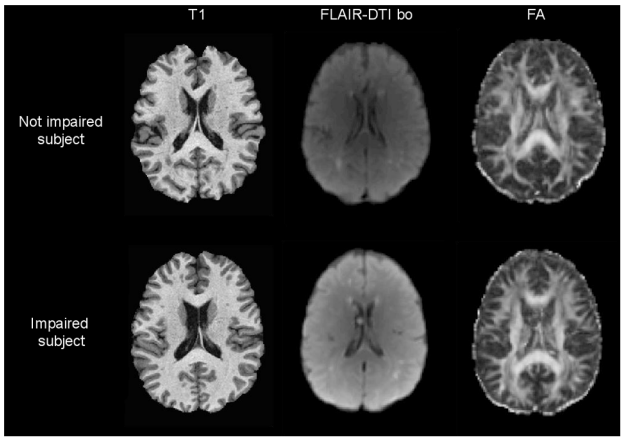

Figure 1. T1 scans, FLAIR DTI-b0 scans and FA maps of participants presenting sparse WM hyperintensities. These subjects are classified 1 on Fazekas scale after visual inspection. One individual example of each group was presented.
doi:10.1371/journal.pone.0066810.g001

direction of the bundle. This physical property is measured across FA. The more the bundle is coherent (compact and organized), the higher FA values are [22]. In order to improve pathophysiological interpretations of the FA results, the source of FA changes and its underlying tissue damage substrates are investigated using recently-described DTI parameters Axial (AD) and Radial Diffusivity (RD). In particular, AD may serve as a surrogate of axon damage whereas RD may serve as a surrogate of myelin pathology [23,24]. In addition, global and regional cortical volumes and thicknesses will be evaluated on classical 3D-T1 to discriminate between central and peripheral effects on motor bundle integrity. All the analyses were performed first on a whole brain voxel-wise framework and were more extensively explored and confirmed using Regions Of Interest (ROIs) analysis, applied on the cortico-spinal tract and motor cortex.

Materials and Methods

Study set-up and design

Construction of subject groups was based on large dataset examining HIV infection, the ANRS CO3 Aquitaine cohort. This investigation constitutes an open, prospective cohort of HIV-1 infected patients [25,26]. All adults 18 years or older who are in- or out-patients of participating hospital wards with HIV-1 infection confirmed by Western blot testing and who have provided informed consent were eligible to be enrolled in the cohort. The study was approved by the ethics committee of the local institution (CPP Bordeaux) and written informed consent was obtained for all participants. A standardized questionnaire captures different types of data: epidemiologic information (age, gender, HIV transmission category), clinical events since last medical contact (whether or not HIV-related), laboratory (plasma HIV-RNA, CD4, haemoglobin, hepatitis B and C serological status, metabolic parameters) and therapeutic treatment (cART, prophylaxis treatment, other treatment). All events are coded according to the International Classification of Diseases 10^{th} revision (ICD10).

Between December 2007 and September 2009, a cross-sectional study in 324 HIV-1 infected adults from the Aquitaine Cohort was performed to assess the frequency of poor locomotor performance, including the evaluation of lower limb muscle performance with the 5STS test [6,27,28]. The 5STS allows for the assessment of lower limb muscle performance and is a reliable clinical tool to assess functional mobility and locomotor disability in adults [28,29]. The 5STS test measures the time required to complete five sit-to-stand cycles at accelerated speed, recorded with a digital stopwatch. The participant sat on a standard armchair (height 45 cm) with the back against the chair and arms crossed in front of the chest. After one practice trial, the participant was instructed to rise, fully stand up and sit down again five consecutive times as fast as possible, without using the arms to push up from the chair. Timing began when the subject's buttocks leave the chair and stopped when the subject was standing up for the 5^{th} time. All subjects were able to perform the test. The test was administered by an experienced physical therapist who systematically used the same verbal procedure. For the 5STS test, poor test performance was defined by a test result of more than 2SD from the expected age-specific mean in the general population [29]. Among the 324 patients included in the locomotor study, 161 patients also had an MRI examination. Participants with dementia, history of opportunistic cerebral infection (*i.e.* toxoplasmosis), history of harmful alcohol or substance use, or absence of cART, were excluded from the present analysis (n = 46). The MRI data for each of the remaining 114 participants was inspected to discard major acquisition artifacts (n = 23), excessive head motion and technical failure during MRI post-treatment process (n = 12), or cerebral pathologies (n = 7). Using Fazekas scale [29], individuals presenting a high white matter lesion load (grade 2 and 3) were also excluded (n = 5). Finally, 86 participants were included in the present analysis, of which 40 were classified as 5STS-impaired, but none presented clinical signs of myopathy. Among the final participants, most had only small focal lesions (see Figure 1).

MRI Acquisition

Two types of MRI scans were acquired using a 1.5 Tesla Intera system (Philips Medical Systems, Netherlands) equipped with a quadrature head coil: (1) Anatomical high resolution MRI scans of $1\times1\times1$ mm^3 using a 3D MPRAGE T1 weighted sequence (TR = 8.5 ms, TE = 3.9 ms, Flip angle = 8°, Matrix size = 256×224, FOV = 256×224 mm^2 with 170 slices of 1 mm to cover the whole brain); (2) DTI scans using three repetitions of a single shot spin-echo EPI FLAIR DTI sequence (TR = 11258 ms, TE = 94 ms, Flip angle = 90°, Matrix size = 128×128, FOV = 226 mm^2 with 150 slices of 2.5 mm, resulting in an acquisition voxel size of $1.77\times1.77\times2.5$ mm^3, b_{value} = 1000s/mm^2, six images with $b_{value} = 0$, 32 directions).

DTI analysis

Microstructural analysis: Tract Based Spatial Statistics (TBSS). Data processing was performed using FSL 4.1.8 software (FMRIB's Software Library; www.fmrib.ox.ac.uk/fsl/). The data were first visually checked to ensure quality of acquisition. For each subject, raw DTI images were pre-processed using Eddy Current correction and a brain mask was created using BET (Brain Extraction Tool). FA, AD and RD maps were computed by fitting a tensor model to the raw diffusion data using FDT (FMRIB's Diffusion Toolbox). TBSS was then used to perform a voxel-wise between-groups analysis of DTI metrics [30]. First, the FMRIB58 template was used as a target for all nonlinear registrations. The aligned FA maps were then averaged to create a mean FA image. Subsequently, classical TBSS processing was used (WM skeleton generation with a threshold FA value of 0.2 and projection of FA values on this skeleton). The same procedure was used to project values of AD and RD on the WM skeleton.

DTI indices extraction in white matter ROIs. Since whole brain voxel-based analysis derived from AD maps

Table 1. Comparison between 5STS impaired and unimpaired subjects.

	Unimpaired 5STS subjects (n = 46)	Impaired 5STS subjects (n = 40)	p value (Student t-test or Fisher's exact test)
age (years)	50.8±10.8	46.5±7.4	**0.033***
men (n,%)	44 (95%)	34 (85%)	0.092
Right-handed (n,%)	42 (91%)	34 (85%)	0.358
HIV-related variables			
current CD4 (mm^3)	600±278	509±220	0.101
Viral Load >50 cop/ml (n,%)	8 (17%)	4 (10%)	0.252
Log Viral Load	1.82±0.67	1.68±0.25	0.187
infection duration (years)	12.22±6.4	14.4±5.8	0.102
CDC stage (n,%)			0.514
A	24 (53%)	21 (53%)	
B	13 (28%)	12 (30%)	0.514
C	9 (19%)	7 (17%)	
Locomotor performances			
5STS (sec)	8.14±1.5	11.7±2.5	**0.000*****
Morphometric parameters			
global GM (cm^3)	645.3±78.1	657.1±71.7	0.47
global WM (cm^3)	505.3±65	503±62	0.871
left precentral volumes (cm^3)	6.22±0.84	6.3±0.82	0.616
left precentral thickness (mm)	2.75±0.14	2.77±0.16	0.609
Structural parameters			
FA left PLIC	0.68±0.02	0.66±0.02	**0.000*****
AD left PLIC (10^{-3} mm^2/sec)	1.39±0.04	1.36±0.03	**0.006****
RD left PLIC (10^{-3} mm^2/sec)	0.58±0.02	0.58±0.01	0.933
FA left temporal cingulum	0.51±0.03	0.50±0.04	0.107
AD left temporal cingulum (10^{-3} mm^2/sec)	3.06±0.39	3.03±0.37	0.711
RD left temporal cingulum (10^{-3} mm^2/sec)	2.47±0.3	2.48±0.3	0.894

Student t-test or Fisher's exact test for demographic, HIV-related variables and locomotor performances. ANCOVA for morphometric and structural parameters with age, sex, laterality as covariables. p<0.05* ; p<0.01**; p<0,001*** (mean± SD).
doi:10.1371/journal.pone.0066810.t001

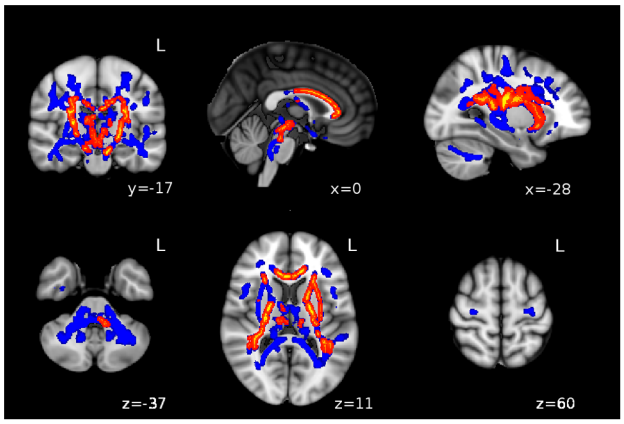

Figure 2. FA decrease in 5STS impaired participants. Highlighted voxels (blue or red) correspond to voxels presenting a significant reduction of FA value in 5STS impaired HIV-infected participants (n = 40) when compared to 5STS unimpaired HIV-infected participants (n = 46). Results are superimposed on MNI template with blue color corresponding to p<0.05, TFCE corrected and red to p<0.01, TFCE corrected. L = left.
doi:10.1371/journal.pone.0066810.g002

highlighted posterior limb of the internal capsule (PLIC), we performed a ROI analysis on this region of the Cortico-Spinal-Tract (CST) bilaterally. Binary masks of the left and right PLIC based on the JHU ICBM-DTI-81 white matter labels atlas provided in FSL were used to extract axial and radial diffusion indices. Moreover, to test the specificity of the observed effects, we extracted AD and RD in ROIs not implicated in motor control, i.e., the left and right temporal cingulum.

Morphometric analysis

Macrostructural analysis: Voxel-Based Morphometry (VBM). An optimized VBM procedure was used to analyze brain volumes [31,32] using the VBM5 toolbox (C. Gaser; http://dbm.neuro.uni-jena.de/vbm) implemented in the Statistical Parametric Software (SPM5, Wellcome Laboratory of the Department of Cognitive Neurology, London, UK, http://www.fil.ion.ucl.ac.uk./spm/). The resulting maps were then smoothed with an isotropic Gaussian filter of 8-mm Full-Width at Half-Maximum (FWHM).

Finally, the Total Intracranial Volume (TIV) was calculated which corresponds to the sum of whole grey, whole white and whole Cerebro-Spinal Fluid (CSF) volumes.

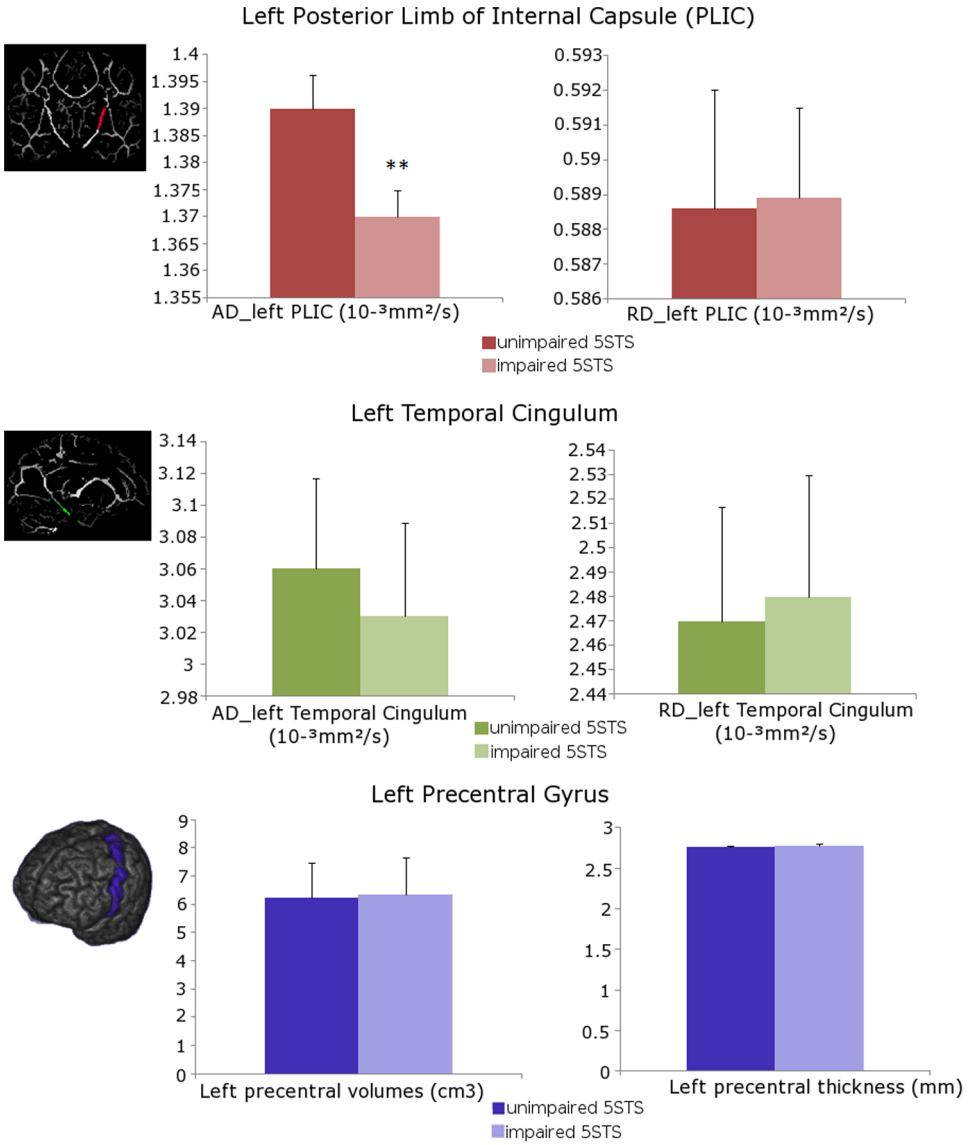

Figure 3. ROI comparisons between 5STS unimpaired (n = 46) and impaired (n = 40) participants. AD and RD of left PLIC (upper raw) and left temporal cingulum (middle raw) and volume and thickness of left precentral region (bottom raw) were compared (ANCOVA with age, sex and laterality as covariables, ** $p<0.01$).
doi:10.1371/journal.pone.0066810.g003

Cortical thickness and volume of ROI. Cortical thickness and volumes of left and right precentral cortices (cortical regions holding central motoneurons) were obtained for each participant using Freesurfer image analysis suite (version 5.1, http://surfer.nmr.mgh.harvard.edu/); [33,34]. Briefly, the processing includes removal of non-brain tissue [35], transformation to Talairach-like space, and segmentation of gray/white matter tissue [36,37]. The entire cortex of each subject was then visually inspected; no subject was discarded for poor segmentation reason. After creation of the cortical representations, the cerebral cortex was parcellated into anatomical structures [38,39].The anatomical labels were mapped to all individual brains for the quantification of average cortical thickness and average volume using automated FreeSurfer tools. In particular, cortical thickness was computed by finding the shortest distance between a given point on the estimated pial surface and the gray/white matter boundary and vice versa and averaging these two values [40].

Statistical analyses

Comparisons between impaired and unimpaired groups were conducted for demographic, locomotor and HIV-1 related variables using Student t-tests or Mann-Whitney tests depending on variable type.

We then performed a classical voxel-based analysis to compare cerebral structures between 5STS-impaired and 5STS-unimpaired participants. Multiple linear regressions in the general linear model were performed on: (a) the FA, AD and RD maps using FSL, with the number of permutations set at 5000 and resulting statistical maps threshold set at least at $p<0.05$, with corrections for multiple comparisons by using the threshold-free cluster enhancement (TFCE); (b) the WM maps at a statistical threshold of $p<0.05$, after corrections for multiple comparisons using false discovery rate (FDR), with an extent threshold of 100 voxels in SPM5. Age, sex, laterality (and TIV when considering volumes) were entered into the models as covariates.

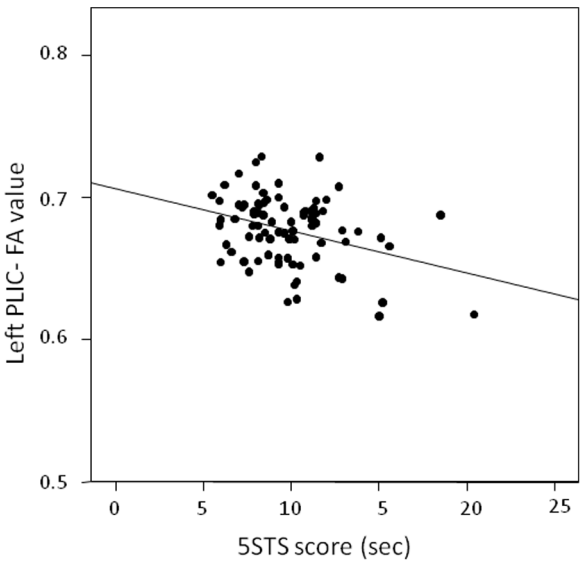

Figure 4. Scatter plot showing correlation between left PLIC-FA values and 5STS score. The analysis includes all participants.
doi:10.1371/journal.pone.0066810.g004

We next conducted statistical analyses on extracted structural parameters of different ROIs using SPSS (16.0.1, SPSS Inc.). ANCOVA was applied with age, sex and laterality as covariables. Pearson correlation analyses were also performed between 5STS scored and DTI indices. In these analyses, p-values below than 0.05 were considered as significant.

Results

Forty participants presented low performance at the 5STS (*i.e.* score greater than 2 standard deviations above the expected age-specific mean in the general population). Mean score at the 5STS for these impaired participants was of 11.7±2.5 sec whereas for unimpaired it was of 8.1±1.5 sec ($t(84) = -7.947$ $p<0.001$) (Table 1). Impaired participants were significantly younger than unimpaired participants (46.5±1.17 years versus 50.8±1.6 years, $p = 0.033$), but they were not different concerning infection duration, CD4 count, viral load or CDC stage at the time of evaluation.

DTI analysis

The voxel-wise analysis performed on FA maps demonstrated that 5STS impaired participants had lower FA values at the level of various tracts and especially at the level of motor tracts, *i.e.* the cortico-spinal tracts (CST), the middle cerebellar peduncles, the medial lemniscus and the corpus callosum (CC) (all differences $p<0.05$, TFCE corrected, Figure 2). It is noteworthy, that impaired participants presented a reduced FA all along the CST, in the midbrain, in the internal capsule and also in the proximal part of CST (the corona radiata close to precentral gyri, which underlies the specificity of the observed relationship). When a more stringent threshold ($p<0.01$, TFCE corrected) was applied, lower FA values persisted in the CST and in the anterior CC (Figure 2). Impaired participants also presented a smaller value of AD at the proximal level of the left CST ($p<0.05$ TFCE corrected), whereas no difference was observed for RD. Subsequent ROI analyses confirmed that impaired participants presented significant lower AD values at the level of the left posterior limb of the internal capsule (PLIC) (1.36±0.03 10^{-3} mm^2/sec) when compared to unimpaired participants (1.39±0.04 10^{-3} mm^2/sec, $F(4,85) = 8.038$, $p = 0.006$). No difference was observed for RD values at this level between impaired and unimpaired participants (0.58±0.01 10^{-3} mm^2/sec *versus* 0.58±0.02 10^{-3} mm^2/sec respectively for, $F(4,85) = 0.38$, $p = 0.539$) (Figure 3). The same results were obtained for the right hemisphere (data not shown). In order to appreciate regional specificity of this difference, we explored the group differences for AD and RD values along the left temporal cingulum, which is not involved in motor control. At the level of this white matter bundle, no difference was detected between unimpaired and impaired participants (3.06±0.39 10^{-3} mm^2/sec *versus* 3.03±0.37 10^{-3} mm^2/sec respectively, for AD values, $F(4,85) = 0.222$, $p = 0.639$, and 2.47±0.3 10^{-3} mm^2/sec *versus* 2.48±0.3 10^{-3} mm^2/sec respectively for RD values, $F(4,85) = 0.918$, $p = 0.341$). A significant correlation was observed between 5STS score and left PLIC- FA values ($r = -0.337$, $p<0.001$, Figure 4) as well with left PLIC-AD values ($r = -0.197$, $p<0.034$).

Morphometric analysis

When global grey or white matter volumes were compared between the two groups, no significant difference was observed. Similarly, no regional differences were observed using VBM analysis comparing the 2 groups.

No difference emerged for comparisons between unimpaired and impaired participants regarding volume (6.22±0.84 cm^3 *versus* 6.30 ±0.82 mm^3 respectively, $F(4,85) = 0.007$, $p = 0.932$) or cortical thicknesses (2.75±0.14 mm^3 *versus* 2.77±0.16 respectively, $F(4,85) = 0.032$, $p = 0.858$) in left precentral regions (Figure 3). In the same way, no difference was observed when right precentral regions were examined (data not shown).

Discussion

The present study shows that HIV-1 participants presenting motor deficits exhibited a selective decrease in the coherence of central motor tracts in the CST, compared to participants without deficits. In contrast, no macrostructural differences were revealed neither in volume nor in thickness of cortical precentral regions (regions holding cellular bodies of motoneurons projecting in CST) between the two groups. Neither age, nor HIV-related clinical variables are related to WM abnormalities. DTI allows examination of WM abnormalities of the motor tracts in these impaired 5STS subjects, in normal appearing WM on conventional MRI. Since no abnormalities in motor grey matter were observed, Wallerian degeneration cannot explain these WM abnormalities.

Voxel-wise analysis, allowing no *a priori* hypothesis on cerebral regions involved, revealed that participants with impaired motor performance also present low FA values bilaterally all along the CST (from its brainstem to its cranial portions). In animal studies [41–43] as in human studies [44–46], quantitative FA measures are believed to reflect axonal density and/or myelin content. No such difference was observed in non-motor tracts (*i.e.* temporal cingulum), this finding supports the specificity of the relationship between peripheral motor deficit and central motor bundle damage. Thus, we could posit that HIV-1 participants with motor deficits also present axonal degeneration and/or dysmyelination of the CST. This finding is in accordance with a number of studies demonstrating a correlation between morphological alterations of the CST and motor disturbances. Ischemic stroke occurring at the level of the CST was associated with Wallerian degeneration of this tract, as revealed through FA measure [47–49]. In Multiple Sclerosis (MS), a disease characterized by focal WM inflammatory lesions, FA of the CST was related to pyramidal functional scores

[50] and muscular weakness [51]. Finally, in Amyotrophic Lateral Sclerosis (ALS), a neurodegenerative process which takes place at the level of motor neuron cell bodies and spreads to WM efferents [52–57], symptom severity is associated with a decrease of FA of CST [55,58–64]. In all these studies, CST damage is related to a top-down neurodegenerative process occurring either after a direct lesion of the central nervous system (stroke or MS) or after motor neuron impairment (ALS). Nevertheless, the assumption of a top-down driven neurodegenerative process is unlikely in our study because locomotor impaired HIV patients with cerebral pathology were excluded from our analysis. In support of this possibility, motor cortex integrity was assumed since neither volume nor thickness decreases were observed in cortical motor areas. Otherwise, the presence of white matter damage specifically in the motor tracts (and nowhere else), and the fact that both HIV-1 groups present comparable viral loads, CD4-count, infection duration and CDC-clinical stage argue against non specific toxic effect of HIV-infection on CST microstructure integrity. This conclusion is also supported by previous observations indicating that neither history of polyneuropathy nor cART treatment are related to 5STS impairment [5]. In sum, these data support the hypothesis that the FA decrease observed in the CST of motor-impaired HIV patients is a central adaptation (mal-adaptative plasticity?) to peripheral impairment, i.e. muscular weakness frequently observed in HIV patients. We could posit that a decrease of muscular exercise due to muscular weakness could induce an adaptation of the supraspinal motor command. Even if the cross-sectional design of our study does not give us access to the dynamic of the FA decrease during the course of the disease, we can speculate that a vicious circle could set in, mutually worsening peripheral muscle weakness and motor central bundle damage. However, we cannot exclude a functional adaptation of neurons of the motor cortex (not evaluated here) associated with a decrease in motor ability [65], which might affect WM efferents and induce a decrease of CST coherence. Also, we cannot exclude the possibility that CST compromise occurs earlier than grey matter atrophy or even that it is an independent phenomenon. Accordingly, a recent brain MRI study performed on myotonic dystrophies revealed large white matter changes which exceed those for grey matter. This observation led the authors to conclude against Wallerian degeneration as the major cause of white matter impairment in this muscular pathology [66].

At this stage, the question arises as to the pathophysiological mechanism underlying white matter tract injury. Whole brain analyses contrasting 5STS unimpaired and impaired motor participants revealed that specific FA decreases observed in 5STS-impaired participants also demonstrate AD decreases at the same level (the left PLIC), while RD remains unchanged in these same individuals. These results were confirmed and extended to right PLIC by ROIs analyses. The FA decrease seems to be driven by a relative AD decrease. According to rodent studies, RD is a fairly consistent biomarker of myelination rates [24,67–72] whereas AD rather reflects axonal changes [41,42,67]. The concomitant decrease of FA and AD could then be driven by a decreased fiber tract organization (caliber change, decreased density and packing of the axons). Even if biological interpretations of the various DTI indices still remain a major concern in the MRI literature [73,74], our results remain consistent with a bottom-up effect.

Methodological considerations

Recently, it has been demonstrated that diffusivity metrics are greatly contaminated by voxels containing CSF due to WM atrophy [75–77]. Our results do not appear to be susceptible to this misinterpretation since locomotor-impaired participants did not present lower WM volumes compared to unimpaired participants. WM hyperintensities have also been shown to impact DTI indices measures [75]. Here again, this interpretation could be discounted since participants included in the study generally presented normal appearing WM.

In conclusion, our results suggest that motor impaired HIV-1 participants present central motor tract disorganization which could be an adaptation to their peripheral impairment rather than a neurodegenerative process. This maladaptative process could support increased damage in white matter bundles throughout the course of the disease and then exacerbate the initial muscular weakness, increasing the risk of falls and disability in these individuals [78,79]. However, given the recent studies on cerebral plasticity following physical training, muscle training in HIV-1 participants may be able to counteract this maladaptive process and may facilitate rehabilitation.

Acknowledgments

The authors wish to thank Joel Swendsen for the English revision of the manuscript.

Composition of the ANRS CO3 Aquitaine Cohort and the Groupe d'Epidemiologie Clinique du SIDA en Aquitaine (GECSA) – Coordination: F. Dabis[1*].

Scientific committee: F. Bonnet[2], F. Dabis[1], M. Dupon[3], G. Chêne[1], H. Fleury[2], D. Lacoste[2], D. Malvy[2], P. Mercié[2], I. Pellegrin[2], P. Morlat[2], D. Neau[2], JL. Pellegrin[2], R. Thiébaut[2], K. Titier[2]. Epidemiology and Methodology: M. Bruyand[1], G. Chêne[1], F. Dabis[1], S. Lawson-Ayayi[1], R. Thiébaut[1], L. Wittkop[1]. Infectious Diseases and Internal Medicine: F. Bonnal[4], F. Bonnet[2], N. Bernard[2], L. Caunègre[2], C. Cazanave[2], J. Ceccaldi[5], D. Chambon[2], I. Chossat[6], K. Courtaud[7], FA. Dauchy[2], S. De Witte[7], M. Dupon[2], A. Dupont[3], P. Duffau[2], H. Dutronc[2], S. Farbos[4], V. Gaboriau[8], MC. Gemain[4], Y. Gerard[2], C. Greib[2], M. Hessamfar[2], D. Lacoste[2], P. Lataste[9], S. Lafarie-Castet[2], E. Lazaro[2], M. Longy-Boursier[2], D. Malvy[2], JP. Meraud[9], P. Mercié[2], E. Monlun[8], P. Morlat[2], D. Neau[2], A. Ochoa[2], JL. Pellegrin[2], T. Pistone[2], JM. Ragnaud[2], MC. Receveur[2], J. Roger-Schmeltz[2], S. Tchamgoué[5], P. Thibaut[2], MA. Vandenhende[2], JF. Viallard[2]. Immunology: JF. Moreau[2], I. Pellegrin[2]. Virology: H. Fleury[2], ME. Lafon[2], B. Masquelier[2], P. Trimoulet[2]. Pharmacology: D. Breilh[2], K. Titier[2]. Drug monitoring: F. Haramburu[2], G. Miremont-Salamé[2]. Data collection and processing: MJ. Blaizeau[2], M. Decoin[2], J. Delaune[1], S. Delveaux[2], C. D'Ivernois[2], C. Hanappier[2], O. Leleux[1], B. Uwamaliya-Nziyumvira[1], X. Sicard[1]. Computing and Statistical analysis: S. Geffard[1], J. Leray[1], G. Palmer[1], D. Touchard[1].

1 Centre de Recherche INSERM U897, Université de Bordeaux, France

2 CHU Bordeaux, France

3 CHG Arcachon, France

4CHG Bayonne, France

5 CHG Libourne, France

6 CHG Villeneuve sur Lot, France

7 CHG de Mont-de-Marsan, France

8 CHG Pau, France

9 CHG Périgueux, France

* Coordinator of the ANRS CO3 Aquitaine study group : François DABIS, ; francois.dabis@isped.u-bordeaux2.fr

Université de Bordeaux, INSERM U 897, ISPED

146 Rue Leo Saignat, 33076 Bordeaux cedex, France.

Tel : +33 (0)557571436

Author Contributions

Conceived and designed the experiments: GC CB PD MA BD HA FD CG FD GECSA-Cogloc. Performed the experiments: GC CB PD MA BD GECSA-Cogloc Study Group. Analyzed the data: GC CB PD MA BD. Contributed reagents/materials/analysis tools: GC CB PD MA BD GECSA-Cogloc Study Group. Wrote the paper: GC CB PD MA BD FB.

References

1. Rusch M, Nixon S, Schilder A, Braitstein P, Chan K, et al. (2004) Impairments, activity limitations and participation restrictions: prevalence and associations among persons living with HIV/AIDS in British Columbia. Health Qual Life Outcomes 2: 46.
2. Robinson-Papp J, Simpson DM (2009) Neuromuscular diseases associated with HIV-1 infection. Muscle Nerve 40: 1043–1053.
3. Navia BA, Jordan BD, Price RW (1986) The AIDS dementia complex: I. Clinical features. Ann Neurol 19: 517–524.
4. (1991) Working Group of the American Academy of Neurology AIDS Task Force. Neurology 41: 778–785.
5. Richert L, Dehail P, Mercie P, Dauchy FA, Bruyand M, et al. (2011) High frequency of poor locomotor performance in HIV-infected patients. AIDS 25: 797–805.
6. Csuka M, McCarty DJ (1985) Simple method for measurement of lower extremity muscle strength. Am J Med 78: 77–81.
7. Nevitt MC, Cummings SR, Kidd S, Black D (1989) Risk factors for recurrent nonsyncopal falls. A prospective study. JAMA 261: 2663–2668.
8. Campbell AJ, Borrie MJ, Spears GF (1989) Risk factors for falls in a community-based prospective study of people 70 years and older. J Gerontol 44: M112–117.
9. Lipsitz LA, Jonsson PV, Kelley MM, Koestner JS (1991) Causes and correlates of recurrent falls in ambulatory frail elderly. J Gerontol 46: M114–122.
10. Stebbins GT, Smith CA, Bartt RE, Kessler HA, Adeyemi OM, et al. (2007) HIV-associated alterations in normal-appearing white matter: a voxel-wise diffusion tensor imaging study. J Acquir Immune Defic Syndr 46: 564–573.
11. Chen Y, An H, Zhu H, Stone T, Smith JK, et al. (2009) White matter abnormalities revealed by diffusion tensor imaging in non-demented and demented HIV+ patients. Neuroimage 47: 1154–1162.
12. Pfefferbaum A, Rosenbloom MJ, Adalsteinsson E, Sullivan EV (2007) Diffusion tensor imaging with quantitative fibre tracking in HIV infection and alcoholism comorbidity: synergistic white matter damage. Brain 130: 48–64.
13. Tate DF, Conley J, Paul RH, Coop K, Zhang S, et al. (2010) Quantitative diffusion tensor imaging tractography metrics are associated with cognitive performance among HIV-infected patients. Brain Imaging Behav 4: 68–79.
14. Sullivan EV, Rosenbloom MJ, Rohlfing T, Kemper CA, Deresinski S, et al. (2011) Pontocerebellar contribution to postural instability and psychomotor slowing in HIV infection without dementia. Brain Imaging Behav 5: 12–24.
15. Authier FJ, Chariot P, Gherardi RK (2005) Skeletal muscle involvement in human immunodeficiency virus (HIV)-infected patients in the era of highly active antiretroviral therapy (HAART). Muscle Nerve 32: 247–260.
16. Dudgeon WD, Phillips KD, Carson JA, Brewer RB, Durstine JL, et al. (2006) Counteracting muscle wasting in HIV-infected individuals. HIV Med 7: 299–310.
17. Scott WB, Oursler KK, Katzel LI, Ryan AS, Russ DW (2007) Central activation, muscle performance, and physical function in men infected with human immunodeficiency virus. Muscle Nerve 36: 374–383.
18. Yarasheski KE, Scherzer R, Kotler DP, Dobs AS, Tien PC, et al. (2011) Age-related skeletal muscle decline is similar in HIV-infected and uninfected individuals. J Gerontol A Biol Sci Med Sci 66: 332–340.
19. Crystal S, Fleishman JA, Hays RD, Shapiro MF, Bozzette SA (2000) Physical and role functioning among persons with HIV: results from a nationally representative survey. Med Care 38: 1210–1223.
20. Basser PJ, Pierpaoli C (1996) Microstructural and physiological features of tissues elucidated by quantitative-diffusion-tensor MRI. J Magn Reson B 111: 209–219.
21. Beaulieu C (2002) The basis of anisotropic water diffusion in the nervous system – a technical review. NMR Biomed 15: 435–455.
22. Le Bihan D, Johansen-Berg H (2012) Diffusion MRI at 25: exploring brain tissue structure and function. Neuroimage 61: 324–341.
23. Irvine KA, Blakemore WF (2006) Age increases axon loss associated with primary demyelination in cuprizone-induced demyelination in C57BL/6 mice. J Neuroimmunol 175: 69–76.
24. Song SK, Yoshino J, Le TQ, Lin SJ, Sun SW, et al. (2005) Demyelination increases radial diffusivity in corpus callosum of mouse brain. Neuroimage 26: 132–140.
25. Thiebaut R, Morlat P, Jacqmin-Gadda H, Neau D, Mercie P, et al. (2000) Clinical progression of HIV-1 infection according to the viral response during the first year of antiretroviral treatment. Groupe d'Epidemiologie du SIDA en Aquitaine (GECSA). AIDS 14: 971–978.
26. Bonnet F, Amieva H, Marquant F, Bernard C, Bruyand M, et al. (2013) Cognitive disorders in HIV-infected patients: are they HIV-related? AIDS 27: 391–400.
27. Lord SR, Murray SM, Chapman K, Munro B, Tiedemann A (2002) Sit-to-stand performance depends on sensation, speed, balance, and psychological status in addition to strength in older people. J Gerontol A Biol Sci Med Sci 57: M539–543.
28. Whitney SL, Wrisley DM, Marchetti GF, Gee MA, Redfern MS, et al. (2005) Clinical measurement of sit-to-stand performance in people with balance disorders: validity of data for the Five-Times-Sit-to-Stand Test. Phys Ther 85: 1034–1045.
29. Fazekas F, Chawluk JB, Alavi A, Hurtig HI, Zimmerman RA (1987) MR signal abnormalities at 1.5 T in Alzheimer's dementia and normal aging. AJR Am J Roentgenol 149: 351–356.
30. Smith SM, Jenkinson M, Johansen-Berg H, Rueckert D, Nichols TE, et al. (2006) Tract-based spatial statistics: voxelwise analysis of multi-subject diffusion data. Neuroimage 31: 1487–1505.
31. Ashburner J, Friston KJ (2000) Voxel-based morphometry – the methods. Neuroimage 11: 805–821.
32. Good CD, Johnsrude IS, Ashburner J, Henson RN, Friston KJ, et al. (2001) A voxel-based morphometric study of ageing in 465 normal adult human brains. Neuroimage 14: 21–36.
33. Dale AM, Fischl B, Sereno MI (1999) Cortical surface-based analysis. I. Segmentation and surface reconstruction. Neuroimage 9: 179–194.
34. Fischl B, Sereno MI, Tootell RB, Dale AM (1999) High-resolution intersubject averaging and a coordinate system for the cortical surface. Hum Brain Mapp 8: 272–284.
35. Segonne F, Dale AM, Busa E, Glessner M, Salat D, et al. (2004) A hybrid approach to the skull stripping problem in MRI. Neuroimage 22: 1060–1075.
36. Fischl B, Salat DH, Busa E, Albert M, Dieterich M, et al. (2002) Whole brain segmentation: automated labeling of neuroanatomical structures in the human brain. Neuron 33: 341–355.
37. Fischl B, Salat DH, van der Kouwe AJ, Makris N, Segonne F, et al. (2004) Sequence-independent segmentation of magnetic resonance images. Neuroimage 23 Suppl 1: S69–84.
38. Desikan RS, Segonne F, Fischl B, Quinn BT, Dickerson BC, et al. (2006) An automated labeling system for subdividing the human cerebral cortex on MRI scans into gyral based regions of interest. Neuroimage 31: 968–980.
39. Fischl B, van der Kouwe A, Destrieux C, Halgren E, Segonne F, et al. (2004) Automatically parcellating the human cerebral cortex. Cereb Cortex 14: 11–22.
40. Fischl B, Dale AM (2000) Measuring the thickness of the human cerebral cortex from magnetic resonance images. Proc Natl Acad Sci U S A 97: 11050–11055.
41. Kim JH, Budde MD, Liang HF, Klein RS, Russell JH, et al. (2006) Detecting axon damage in spinal cord from a mouse model of multiple sclerosis. Neurobiol Dis 21: 626–632.
42. DeBoy CA, Zhang J, Dike S, Shats I, Jones M, et al. (2007) High resolution diffusion tensor imaging of axonal damage in focal inflammatory and demyelinating lesions in rat spinal cord. Brain 130: 2199–2210.
43. Zhang J, Jones M, DeBoy CA, Reich DS, Farrell JA, et al. (2009) Diffusion tensor magnetic resonance imaging of Wallerian degeneration in rat spinal cord after dorsal root axotomy. J Neurosci 29: 3160–3171.
44. Madler B, Drabycz SA, Kolind SH, Whittall KP, MacKay AL (2008) Is diffusion anisotropy an accurate monitor of myelination? Correlation of multicomponent T2 relaxation and diffusion tensor anisotropy in human brain. Magn Reson Imaging 26: 874–888.
45. Concha L, Livy DJ, Beaulieu C, Wheatley BM, Gross DW (2010) In vivo diffusion tensor imaging and histopathology of the fimbria-fornix in temporal lobe epilepsy. J Neurosci 30: 996–1002.
46. Klawiter EC, Schmidt RE, Trinkaus K, Liang HF, Budde MD, et al. (2011) Radial diffusivity predicts demyelination in ex vivo multiple sclerosis spinal cords. Neuroimage 55: 1454–1460.
47. Wieshmann UC, Symm MR, Bartlett PA, Shorvon SD, Clark CA, et al. (1999) Diffusion weighted MRI demonstrates abnormal pyramidal tract in hemiparesis. J Neurol Neurosurg Psychiatry 66: 797–798.
48. Werring DJ, Toosy AT, Clark CA, Parker GJ, Barker GJ, et al. (2000) Diffusion tensor imaging can detect and quantify corticospinal tract degeneration after stroke. J Neurol Neurosurg Psychiatry 69: 269–272.
49. Kunimatsu A, Aoki S, Masutani Y, Abe O, Hayashi N, et al. (2004) The optimal trackability threshold of fractional anisotropy for diffusion tensor tractography of the corticospinal tract. Magn Reson Med Sci 3: 11–17.
50. Wilson M, Tench CR, Morgan PS, Blumhardt LD (2003) Pyramidal tract mapping by diffusion tensor magnetic resonance imaging in multiple sclerosis: improving correlations with disability. J Neurol Neurosurg Psychiatry 74: 203–207.
51. Reich DS, Zackowski KM, Gordon-Lipkin EM, Smith SA, Chodkowski BA, et al. (2008) Corticospinal tract abnormalities are associated with weakness in multiple sclerosis. AJNR Am J Neuroradiol 29: 333–339.
52. Roccatagliata L, Bonzano L, Mancardi G, Canepa C, Caponnetto C (2009) Detection of motor cortex thinning and corticospinal tract involvement by quantitative MRI in amyotrophic lateral sclerosis. Amyotroph Lateral Scler 10: 47–52.
53. Verstraete E, van den Heuvel MP, Veldink JH, Blanken N, Mandl RC, et al. (2010) Motor network degeneration in amyotrophic lateral sclerosis: a structural and functional connectivity study. PLoS One 5: e13664.
54. Verstraete E, Veldink JH, Mandl RC, van den Berg LH, van den Heuvel MP (2011) Impaired structural motor connectome in amyotrophic lateral sclerosis. PLoS One 6: e24239.
55. Rose S, Pannek K, Bell C, Baumann F, Hutchinson N, et al. (2012) Direct evidence of intra- and interhemispheric corticomotor network degeneration in amyotrophic lateral sclerosis: An automated MRI structural connectivity study. Neuroimage 59: 2661–2669.
56. Turner MR, Hammers A, Allsop J, Al-Chalabi A, Shaw CE, et al. (2007) Volumetric cortical loss in sporadic and familial amyotrophic lateral sclerosis. Amyotroph Lateral Scler 8: 343–347.

57. Turner MR, Kiernan MC, Leigh PN, Talbot K (2009) Biomarkers in amyotrophic lateral sclerosis. Lancet Neurol 8: 94–109.
58. Sage CA, Peeters RR, Gorner A, Robberecht W, Sunaert S (2007) Quantitative diffusion tensor imaging in amyotrophic lateral sclerosis. Neuroimage 34: 486–499.
59. Ellis CM, Simmons A, Jones DK, Bland J, Dawson JM, et al. (1999) Diffusion tensor MRI assesses corticospinal tract damage in ALS. Neurology 53: 1051–1058.
60. Toosy AT, Werring DJ, Orrell RW, Howard RS, King MD, et al. (2003) Diffusion tensor imaging detects corticospinal tract involvement at multiple levels in amyotrophic lateral sclerosis. J Neurol Neurosurg Psychiatry 74: 1250–1257.
61. Unrath A, Muller HP, Riecker A, Ludolph AC, Sperfeld AD, et al. (2010) Whole brain-based analysis of regional white matter tract alterations in rare motor neuron diseases by diffusion tensor imaging. Hum Brain Mapp 31: 1727–1740.
62. Iwata NK, Aoki S, Okabe S, Arai N, Terao Y, et al. (2008) Evaluation of corticospinal tracts in ALS with diffusion tensor MRI and brainstem stimulation. Neurology 70: 528–532.
63. Blain CR, Williams VC, Johnston C, Stanton BR, Ganesalingam J, et al. (2007) A longitudinal study of diffusion tensor MRI in ALS. Amyotroph Lateral Scler 8: 348–355.
64. Ciccarelli O, Behrens TE, Johansen-Berg H, Talbot K, Orrell RW, et al. (2009) Investigation of white matter pathology in ALS and PLS using tract-based spatial statistics. Hum Brain Mapp 30: 615–624.
65. Adkins DL, Boychuk J, Remple MS, Kleim JA (2006) Motor training induces experience-specific patterns of plasticity across motor cortex and spinal cord. J Appl Physiol 101: 1776–1782.
66. Minnerop M, Weber B, Schoene-Bake JC, Roeske S, Mirbach S, et al. (2011) The brain in myotonic dystrophy 1 and 2: evidence for a predominant white matter disease. Brain 134: 3530–3546.
67. Song SK, Sun SW, Ramsbottom MJ, Chang C, Russell J, et al. (2002) Dysmyelination revealed through MRI as increased radial (but unchanged axial) diffusion of water. Neuroimage 17: 1429–1436.
68. Budde MD, Xie M, Cross AH, Song SK (2009) Axial diffusivity is the primary correlate of axonal injury in the experimental autoimmune encephalomyelitis spinal cord: a quantitative pixelwise analysis. J Neurosci 29: 2805–2813.
69. Harsan LA, Poulet P, Guignard B, Steibel J, Parizel N, et al. (2006) Brain dysmyelination and recovery assessment by noninvasive in vivo diffusion tensor magnetic resonance imaging. J Neurosci Res 83: 392–402.
70. Harsan LA, Poulet P, Guignard B, Parizel N, Skoff RP, et al. (2007) Astrocytic hypertrophy in dysmyelination influences the diffusion anisotropy of white matter. J Neurosci Res 85: 935–944.
71. Tyszka JM, Readhead C, Bearer EL, Pautler RG, Jacobs RE (2006) Statistical diffusion tensor histology reveals regional dysmyelination effects in the shiverer mouse mutant. Neuroimage 29: 1058–1065.
72. Wu YC, Field AS, Duncan ID, Samsonov AA, Kondo Y, et al. (2011) High b-value and diffusion tensor imaging in a canine model of dysmyelination and brain maturation. Neuroimage 58: 829–837.
73. Budde MD, Frank JA (2012) Examining brain microstructure using structure tensor analysis of histological sections. Neuroimage 63: 1–10.
74. Wheeler-Kingshott CA, Cercignani M (2009) About "axial" and "radial" diffusivities. Magn Reson Med 61: 1255–1260.
75. Vernooij MW, de Groot M, van der Lugt A, Ikram MA, Krestin GP, et al. (2008) White matter atrophy and lesion formation explain the loss of structural integrity of white matter in aging. Neuroimage 43: 470–477.
76. Bosch B, Arenaza-Urquijo EM, Rami L, Sala-Llonch R, Junque C, et al. (2012) Multiple DTI index analysis in normal aging, amnestic MCI and AD. Relationship with neuropsychological performance. Neurobiol Aging 33: 61–74.
77. Hugenschmidt CE, Peiffer AM, Kraft RA, Casanova R, Deibler AR, et al. (2008) Relating imaging indices of white matter integrity and volume in healthy older adults. Cereb Cortex 18: 433–442.
78. Guralnik JM, Ferrucci L, Simonsick EM, Salive ME, Wallace RB (1995) Lower-extremity function in persons over the age of 70 years as a predictor of subsequent disability. N Engl J Med 332: 556–561.
79. Buatois S, Miljkovic D, Manckoundia P, Gueguen R, Miget P, et al. (2008) Five times sit to stand test is a predictor of recurrent falls in healthy community-living subjects aged 65 and older. J Am Geriatr Soc 56: 1575–1577.